Proceedings of ASME 2005
ASME TURBO EXPO 2005
June 6-9, 2005, Reno, Nevada

GT2005-68349

CONCEPTUAL DESIGN OF A SUPERSONIC CO_2 COMPRESSOR

Shawn P. Lawlor[♦], **Peter Baldwin**

Ramgen Power Systems
Bellevue, WA
(425) 828-4919

ABSTRACT

Ramgen Power Systems, Inc. (RPS) is developing a family of high performance supersonic compressors that combine many of the aspects of shock compression systems commonly used in supersonic flight inlets with turbo-machinery design practices employed in conventional axial and centrifugal compressor design. The result is a high efficiency compressor that is capable of single stage pressure ratios in excess of those available in existing axial or centrifugal compressors. A variety of design configurations for land-based compressors utilizing this system have been explored.

A proof-of-concept system has been designed to demonstrate the basic operational characteristics of this family of compressors when operating on air. The test unit was designed to process ~1.43 kg/s and produce a pressure ratio across the supersonic rotor of 2.41:1. Based on the results from that effort a compressor specifically designed for the high pressure ratios required to support CO_2 liquification has been proposed. The basic theory of operation of this new family of compressors will be reviewed along with the performance characteristics and conceptual design features of the proposed CO_2 compressor systems. *Keywords:* Compressor, Inlets, Supersonic, CO_2.

INTRODUCTION

A proof-of-concept version of a new type of compression system has been designed, developed and tested. This system applies supersonic aerodynamic design practices that are common in flight propulsion applications to the land based compression of a working gas. The result is an axial flow supersonic compression stage with uniquely low blade counts and shallow blade angles. An additional feature seldom applied in either axial or centrifugal stages is the use of "on-rotor" boundary layer bleed for gas path starting and performance optimization. This technique, referred to by compressor designers such as Kerrebrock [1], as aspiration has been proposed as a method for minimizing shock-boundary layer interactions and associated boundary layer separation. Since the bleed flow is removed from the compressive gas path after experiencing various levels of compression, the treatment of this bleed flow must be carefully considered from a performance perspective so that its impact on the integrated system performance and efficiency levels is properly understood.

The prototype system was designed to demonstrate the basic operational characteristics of this family of compressors when operating on air. Once the modeling techniques, operational characteristics and basic performance potential of the system have been demonstrated, the technology can be applied to a wide range of working gasses and compression levels. The basic theory, design and performance of the prototype system will be discussed in this paper.

The test unit was designed to operate with an inlet relative Mach number of 1.6, process ~1.43 kg/s and produce a pressure ratio across the rotor of 2.41:1. Based on analytical predictions and design studies, supersonic compressor stages, when operating at higher inlet relative Mach numbers, have the potential to deliver higher single stage pressure ratios at greater efficiencies than either axial or centrifugal compressor stages.

Using the design techniques and practices validated by this effort, an industrial CO_2 compressor has been proposed that would offer significant cost savings and efficiency advantages over other CO_2 compressor systems typically used for industrial applications.

♦ Corresponding Author, Chief Technology Officer: slawlor@ramgen.com

NOMENCLATURE

a	speed of sound;	*w*	work
P	pressure,	h	enthalpy
M	Mach number,	V	velocity
T	temperature		
PR	pressure ratio (total/total)		
N_s	compressor specific speed		

Greek Symbols

γ	ratio of specific heats
η_{adb}	adiabatic compressor efficiency
ρ	density
π_{pt}	total pressure recovery
ΔT_{act}	actual temperature change
ΔT_{adb}	adiabatic temperature change

Subscripts

axial	denotes axial direction
rel	denotes relative flow
stage	denotes overall stage
tan	denotes tangential direction
ad	adiabatic
t	total condition
0	free stream condition
1	flow entering compressor
2a	flow leaving compressor - actual
2i	flow leaving compressor – ideal
i	denotes inflow conditions
e	denotes outflow conditions

THEORY OF OPERATION

While supersonic axial compressor stages have been suggested by a number of other investigators [2-6], those rotor stages have invariably been configured so as to resemble conventional axial flow rotors. They have relatively high blade counts and inefficient shock systems generated by the blade surfaces.

In the present case, the rotor was configured with an oblique shock system and terminal normal shock using the design guidelines typically employed in supersonic flight inlet design. By using this approach, it was anticipated that proven performance characteristics for the supersonic flight inlet systems would serve as a basis for the design.

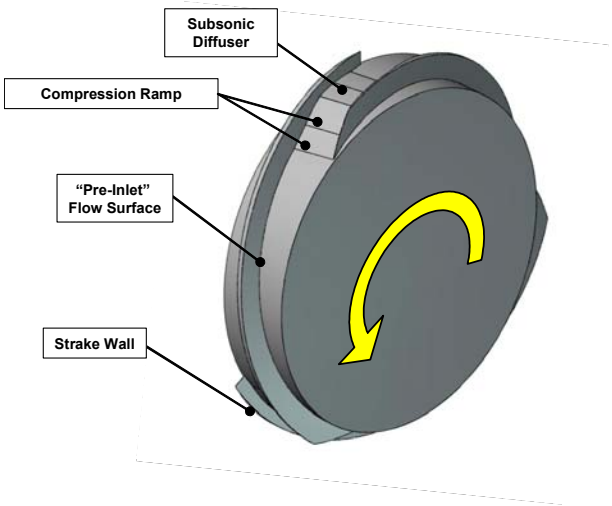

Figure 1. Supersonic Compression Stage Rotor

The supersonic rotor flow-path is formed by three elongated blades or strakes mounted on the rim of the rotor. These strakes are mounted on the rotor at a shallow angle, typically 5° – 10°, and form the axial boundaries of each of the three flow-paths as shown in Figure 1. The strakes themselves are meant to do a minimum of compressive work. The principal shock system is generated by a compressive ramp or largely planar surface integrated into the rim of the rotor. The ramp is developed so as to create a series of oblique shock waves that are reflected by the non-rotating compressor case as shown in Figure 2 (lower).

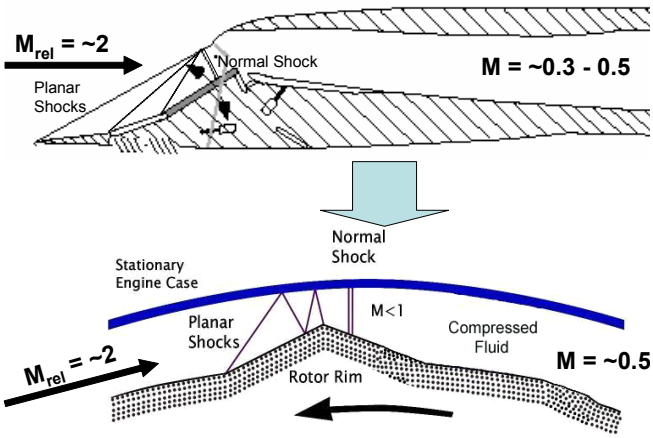

Figure 2. Flight Inlet Schematic (upper), Shock Structure in Test Rig (lower)

This configuration forms a rectangular flow-path with an inflow Mach number that is determined by the rotation rate of the rotor and any swirl that is imparted into the flow upstream of the rotor. Figure 3 shows an unwrapped view of the rotor together with the pre-swirl cascade used to establish the rotor inflow field. In the present case, the design rotor speed was 21,100 rpm. Figure 3 defines the basic flow-path stations surrounding the rotor. Note that stations 2.4 and 2.7 are in the non-rotating, or inertial, reference frame upstream and

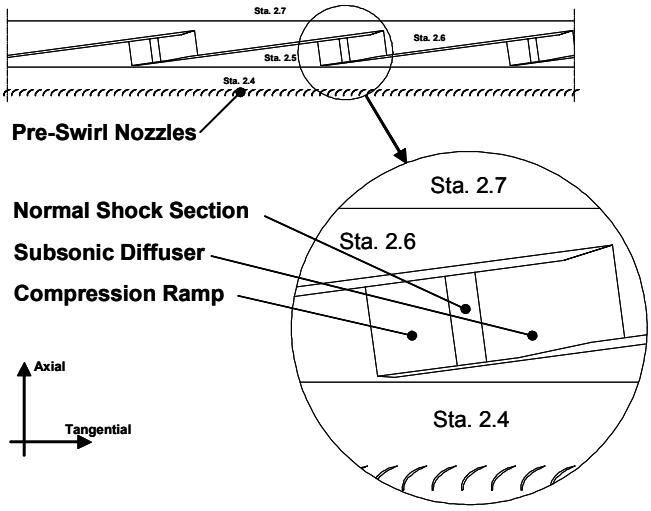

Figure 3. Rotor Station Numbering Convention

downstream of the rotor, respectively. Stations 2.5 and 2.6 are at the rotor inflow and discharge in the rotating, or relative, reference frame. The direction of rotation of the rim shown in Figure 3 is right to left. The combination of the rotor speed and the pre-swirl from the upstream cascade of pre-swirl nozzles created a rotor inflow that was supersonic relative to the moving rotor. The details of the flow-field are summarized in Table 1.

The pattern of shock waves shown in Figure 2 (lower) is comparable to the pattern of shock waves that might be found in a supersonic inlet as would be applied to a missile or supersonic aircraft. A schematic illustration of a typical planar 2-D supersonic inlet as would be applied on an aircraft or missile is shown in Figure 2 (upper) along with the associated oblique and normal shock waves. The shock forming compression ramp of this flight inlet is analogous to the shock forming ramp on the rim of the supersonic compression rotor shown schematically in Figure 2 (lower).

Table 1. Rotor Inflow Conditions

Rotor Speed	***(rpm)***	21,100
Shroud Radius	***(m)***	0.1451
Rim Radius	***(m)***	0.1451
Mass Flow	***(kg/s)***	1.43

Property \ ***Reference Frame***		***Inertial Reference Frame***	***Relative Reference Frame***
P	***(kPa)***	104.60	104.60
T	***(K)***	262	262
ρ	***(kg/m^3)***	1.396	1.396
M	***(---)***	0.70	1.61
V	***(m/s)***	226.7	512.3
V_{axial}	***(m/s)***	69.2	69.2
V_{tan}	***(m/s)***	215.8	516.7
P_t	***(kPa)***	145.14	452.24
T_t	***(K)***	287	398

In the case of a supersonic inlet for flight applications, the total pressure available in the approaching stream-tube can be expressed in terms of the approach Mach number (relative to the inlet) by the familiar expression.

$$P_t = P(1+\frac{\gamma-1}{2}M_0^2)^{\frac{\gamma}{\gamma-1}} \quad (1)$$

For inlet relative Mach numbers ranging from 1.5 to 3.5 it is common practice to design the inlet so as to establish a series of oblique shock waves that decelerate the supersonic flow entering the inlet inflow plane from the inlet relative Mach number to a pre-normal shock Mach number of ~1.3 (Seddon and Goldsmith [7], Mahoney [8]). The losses of these shock systems are functions of the inflow Mach numbers and the turning angles associated with each shock wave. Rough guidelines have emerged to quantify the anticipated losses of supersonic inlets designed for operation at various Mach numbers (Billig and Van Wie [9]). Losses for such inlets are often expressed in terms of total pressure recovery π_{Pt}. The total pressure recovery is a commonly used flight inlet performance metric that is applied when the temperature increases resulting from the compression process are low enough that the gas can be considered as ideal and calorically perfect throughout the process (constant γ). When a calorically imperfect or non-ideal gas is considered, it becomes important to use a different inlet performance metric.

The following relations show conservative guidelines for flight inlet performance levels in terms π_{Pt} for military and commercial flight inlet systems.

$$\pi_{Pt} = 1 - 0.075(M_0 - 1)^{1.35} \quad (2)$$

$$\pi_{Pt} = 1 - 0.1(M_0 - 1)^{1.5} \quad (3)$$

Equations 1, 2 and 3 are shown in Figure 4 along with performance levels for a range of flight inlets. These relations should be viewed as general guidelines only and are strongly influenced by the mission requirements for the associated flight systems. Stable operation over a wide flight Mach Number range as well as roll, pitch and yaw attitudes can impose serious performance penalties on a flight system. For any given operating Mach number, superior performance can be achieved by optimizing a design for operation at a single inlet relative Mach number with no significant inflow perturbations. Point A in Figure 4 is shows the measured performance for a mixed compression inlet designed for a flight Mach number of 2.70 (Wasserbauer et al., [10]) and illustrates the margin for improvement over the "Military Standard" curve that is available when a design is optimized for a given operating condition.

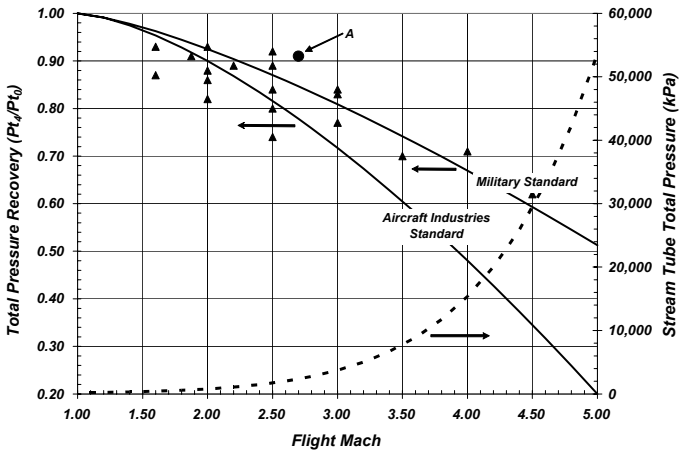

Figure 4. Flight Inlet Performance Characteristics

To put the compression process efficiency implications of Figure 4 into perspective consider the point A on Figure 4. At a flight Mach number of 2.7 the stream tube captured by the inlet would have a total pressure (due to its relative Mach number) of Approximately 23.3 times the free stream static pressure. When tested at a relative Mach number of 2.7, the inlet achieved a total pressure recovery of 0.91. Thus, using a combination of oblique and normal shock waves the inlet was

able to recover 91% of the total pressure in the captured stream tube while decelerating the flow from a Mach number of 2.7 to 0.5. In it's own moving, or relative, reference frame the inlet alone achieved a useable compression ratio of 16.6:1 based on static pressures. To a non-moving observer on the ground, in an inertial reference frame, the air processed by the inlet increased in total pressure by 21.2 times.

Figure 4 shows that when properly designed, supersonic flight inlets can deliver compression ratios ranging from 2.0:1 to 30:1 depending on flight Mach number and total pressure recovery. Moreover, if the efficiency levels indicated in Figure 4 for supersonic flight inlet systems could be achieved in a ground based compression system, such a system would achieve peak efficiency levels superior to many conventional (axial & centrifugal) compression systems operating at comparable pressure ratios. To illustrate this point it is necessary to present the performance of supersonic flight inlets in terms of a performance metric that is typically used to characterize the efficiency of conventional compressors.

The performance of most conventional compressors is often expressed in terms of the adiabatic compression efficiency, η_{ad}. The definition of adiabatic compression efficiency is shown in Equation 4. With further ideal gas assumptions Equation 7 follows as the standard form used by many turbo-machinery designers where changes in temperate and pressure typically relate to total conditions.

Flight inlet performance analysis is typically performed in a reference frame that moves along with, or is relative to, the moving inlet. When viewed in this way there is no change in total enthalpy as the captured stream tube is processed by the inlet and therefore the adiabatic compression efficiency as defined by Equation 4 has little meaning. If, however, a moving flight inlet is viewed not in the moving, or relative, reference frame, but from a stationary reference frame, then there is a change in total enthalpy as the air is processed by the inlet and the performance of the inlet can be expressed in terms of adiabatic compression efficiency. Figure 5 shows the overall compression ratio that would result from the "Military Standard" performance levels illustrated in Figure 4. In Figure 5, the necessary reference frame conversions have been made so as to express the flight inlet performance shown in Figure 4 in terms of η_{ad}.

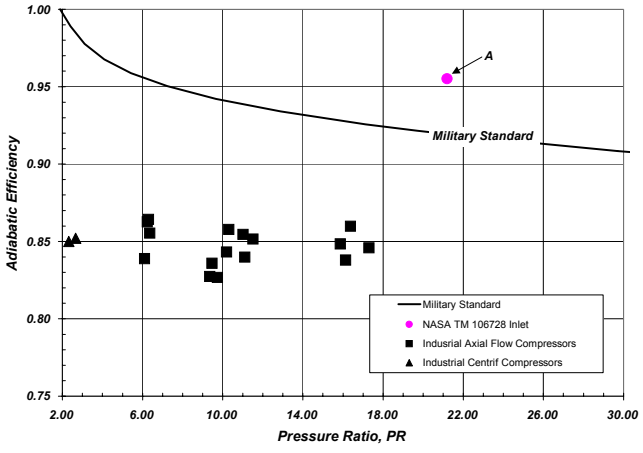

Figure 5. Flight Inlet Performance in Terms of η_{ad}

The adiabatic efficiency levels shown in Figure 5 for Point A and the "Military Standard" performance trend do not include any of the pre-swirl, de-swirl or diffusion losses typically associated with the stator elements in a ground based axial or centrifugal compressor. Efficiently achieving the post supersonic rotor de-swirl and/or diffusion required for various applications is critical to realizing the potential performance advantages suggested in Figure 5.

To illustrate this point, the performance levels for a number of axial flow compressors used on industrial gas turbines (solid squares) have been plotted on Figure 5 as well as a few performance points for lower pressure ratio centrifugal stages used in existing multi-stage inter-cooled air turbo-compressor systems (solid triangles).

$$\eta_{ad} = \frac{w_{2i}}{w_{2a}} = \frac{h_{t2i} - h_{t1}}{h_{t2a} - h_{t1}} \tag{4}$$

$$\eta_{ad} = \frac{\Delta T_{adb}}{\Delta T_{act}} \tag{5}$$

For an ideal, calorically perfect gas the increase in temperature due to an adiabatic compression process of pressure ratio PR can be described as follows.

$$\Delta T_{adb} = T_1 \left(PR^{\frac{\gamma}{(\gamma-1)}} - 1 \right) \tag{6}$$

So that the adiabatic compression efficiency for a calorically perfect gas can be expressed as

$$\eta_{adb} = \frac{T_1 \left(PR^{\frac{\gamma}{(\gamma-1)}} - 1 \right)}{\Delta T_{act}} \tag{7}$$

GENERAL COMPRESSOR CHARACTERISTICS

Just as in the case of supersonic flight inlets, centrifugal, axial flow and rotary positive displacement compression systems have been refined and improved for many decades. The result is a family of mature technologies for the compression of various working gasses. Figure 6 shows the range of expected efficiency levels for these types of compressors. In Figure 6, adiabatic efficiency is plotted against compressor specific speed (Japikse [10]). Since the definition of compressor specific speed includes rotor rotation rate, flow rate and pressure ratio it is a valuable metric for comparison of different compressor technologies. Despite the wide range of performance levels that may be achieved for any specific design, it is clear from Figure 6, that different types of compressors emerge as being particularly well suited for certain ranges of flow, pressure ratio and mechanical speed.

Also shown on Figure 6 are the peak measured and predicted rotor only performance levels for the rig tests completed to date. The performance predicted with the RPS performance model is shown as a solid circle and two data

points showing the highest measured performance levels appear as open triangles.

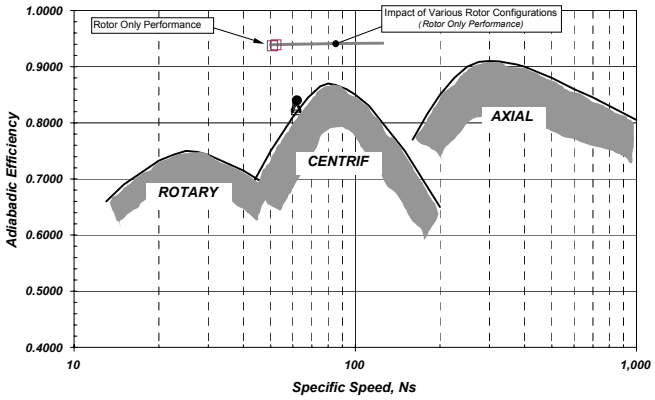

Figure 6. Compressor Performance Comparison

The goal of the current tests has been to demonstrate the basic operability of the design including starting, surge characteristics, sensitivity to bleed, sensitivity to tip gap and the ability of the analysis/design methodology to predict the behavior of the system. It was not the goal of this rig to achieve optimized system performance.

An important feature of the supersonic rotor is that its compression efficiency increases with increasing rotor speed. The loss levels for any required upstream pre-swirl and/or downstream de-swirl stages may have a negative impact on the overall system performance with increasing rotor speed, but the compression efficiency of the supersonic stage increases with increasing rotor speed. In order to realize more of the potential of the system, follow-on tests are planned at higher rotor speeds. Based on performance modeling, these higher pressure ratio, higher speed systems have the potential to achieve increased efficiency levels provided that upstream pre-swirl and downstream de-swirl losses can be minimized.

A higher pressure-ratio rig has been proposed and the design process for that system is underway. The goal for that design is to demonstrate a supersonic stage capable of total pressure ratio's across the supersonic wheel of ~11:1. This supersonic stage is being designed for a relative Mach number of ~2.4. It is intended that this rotor, when coupled with a well designed de-swirl/diffuser would produce an overall system pressure ratio of 9.9:1. The predicted performance levels for the supersonic rotor that would meet the requirements for such a design appear on Figure 6 as open squares. The design of the inlet easily lends itself to increasing capture area and resulting mass flow of the system. The resulting rotor only performance trend is illustrated in Figure 6 by a gray line. These efficiency levels are projected for a supersonic rotor operating so as to produce an inlet relative Mach number of ~2.4 and are for the rotor only, no pre-swirl, de-swirl or other system losses are included.

RAMPRESSOR PERFORMANCE MODELING

The potential design point performance levels for the test rig were modeled using an analytical performance tool that divides the entire compressor flow-path into a series of sections and then applies loss levels to each section. Using the input losses for each section, the program then calculates mean line mass average flow properties at the entrance and exit of each section while conserving mass, momentum and energy relations between each station. In this way the performance tool steps thorough the flow-path integrating the loss effects along the way while conserving mass, momentum, energy and rothalpy relations as appropriate. The result is a set of gas-path properties at each station through the compressor flow-path that are used in the design process and also to predict system discharge conditions. With the inflow and outflow conditions, the overall performance of the system is calculated for use in general design optimization studies as well as comparison to competing technologies.

When possible, results from similar component flow-field tests are used to develop loss levels. When applicable experimental results are not available, various analytical tools including 3-D viscous numerical simulations are used to develop component loss levels for use as inputs to the 1-D performance model. The 1-D performance model has been developed internally by RPS – a detailed presentation of the model is beyond the scope of this paper

One of the important goals for the rig was to validate the design methodology and predictive tools used to design this type of compression system. In addition, the performance and stability of the supersonic shock compression system was to be investigated. No effort was made to optimize the performance of the pre-swirl system or recover any of the pressure in the highly swirling rotor discharge flow. As a result, most of the performance levels and measurements discussed in the following section relate to the property changes across the supersonic rotor only. Table 3 summarizes the flow-path properties predicted by the performance code at key stations upstream and downstream of the supersonic rotor (station numbering convention introduced in Figure 3.). In the case of stations 2.5 and 2.6, the changes that occur between the inflow to the station and the outflow from the station are presented in Table 3 by use of the subscripts ***i*** and ***e*** for inflow and exit respectively.

Table 3. Basic Flow-Path Properties

Property \ Station		2.4 (Inertial)	2.5_i (Relative)	2.6_e (Relative)	2.7 (Inertial)
P	(kPa)	104.6	104.6	331.0	331.0
T	(K)	262.0	262.0	379.0	379.0
M		0.70	1.61	0.49	0.29
a	(m/s)	324.0	324.0	389.6	389.7
V	(m/s)	226.7	521.3	190.0	111.4
V_{axial}	(m/s)	69.2	69.2	25.3	33.1
V_{tan}	(m/s)	215.8	516.7	189.2	0.0
P_t	(kPa)	145.1	452.2	391.0	350.3
T_t	(K)	287.0	398.0	398.0	384.9

Using the pressure and temperature changes across the rotor, the efficiency of the process can be calculated as shown by Equation 7. Based on these mass-averaged one-dimensional properties, the efficiency of the supersonic rotor flow-path was calculated and the design speed, full pressure, rotor only adiabatic efficiency appears as a solid circle in Figure 6. The predicted efficiency is plotted as a function of specific speed. Developing performance levels at decreased pressure levels and

rotor speeds is not straightforward. Numerical simulations have been used to attempt to address a number of off-design performance characteristic. Those results are beyond the scope of this paper.

TEST RESULTS

There are a number of areas that require special attention in the design of this system. Understanding the sensitivity of the system to these issues was a high priority in the test program. The pressure ratio of this stage is high compared to most axial flow stages. As a result, the potential for tip leakage from the high pressure side of the strake to the low pressure side to disrupt the flow-field in the relatively long pre-inlet section leading into the shock compression ramp is an area of particular concern. Attempts were made to characterize these losses using numerical simulations as well are more simplified analytical models. The resulting loss levels were included in the performance model.

The test rig included a thermally controlled tip clearance control ring. The inside diameter of the ring was coated with an abradable material that was intended to be rubbed by the strake tips to achieve the smallest possible tip gap and therefore minimize tip leakage. The tip ring was heated, generating a relatively large tip gap, during the starting process and then the level of tip heating was decreased or the tip ring was actively cooled using cryogenic N_2 to minimize the tip gap when at full speed. One clear result of the test program was that the performance was highly dependant on tip gap and tip leakage.

Another issue that was of concern was the performance of the system during maximum backpressure conditions. In both axial and centrifugal compressors, the phenomenon of surge is encountered when the back-pressure is increased beyond peak levels. In some cases this surge can be violent and result in serious dynamic loads on the system. As a result, most compressor test programs include the investigation and definition of stability limits and the characterization of the stability of operation beyond these limits. In the case of supersonic flight inlets, when maximum allowable back-pressure levels are exceeded the shock system in the inlet can be completely destabilized and collapsed resulting in a process often referred to as "un-start". Under certain conditions supersonic inlet un-start events can be quite violent.

Thus, the stability characteristics of the supersonic rotor when operating at, and beyond peak compression levels received a significant amount of attention. The result of these tests was that the supersonic flow-paths in the rotor had very benign un-start characteristics. As the compression level was increased, the mass flow of the system remained nearly constant resulting in a largely vertical compressor characteristic. As the maximum compression levels were approached mass flow would begin to drop off as the terminal normal shock was pushed upstream of the throat and onto the compression ramp. Once the normal shock progressed onto the ramp the bleed holes on the ramp allowed an increase in bleed to account for the decreased ability of the flow-path minimum area section to pass the captured mass flow. In this fashion the shock was pushed progressively farther toward the inlet capture plane as back-pressure was increased. This process occurred in a smooth and continuous process resulting in a continuous decrease in mass flow until finally after a significant decrease in system mass flow, vibration levels would begin to increase owing to the fundamentally unstable nature of the completely un-started inlet flow-field.

The decrease in mass flow with increasing pressure is shown in Figure 7, which shows compressor characteristics at speeds ranging from 30% to 110%. These characteristics were generated with relatively tight tip clearances. The lower speed lines were extrapolated from limited data. Many other sensitivities and trade studies were performed but a complete presentation of the results is beyond the scope of this paper.

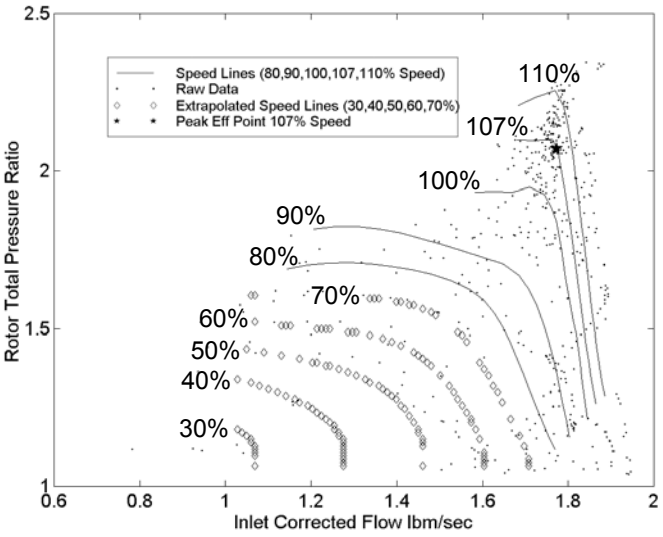

Figure 7. Compressor Speed Lines

Figure 8 shows a plot of rotor-only, or gas-path, efficiency as a function of inlet corrected flow for a number of different rotor speeds. The efficiency levels shown here do not include the losses to the system due to the bleed gas removed from the

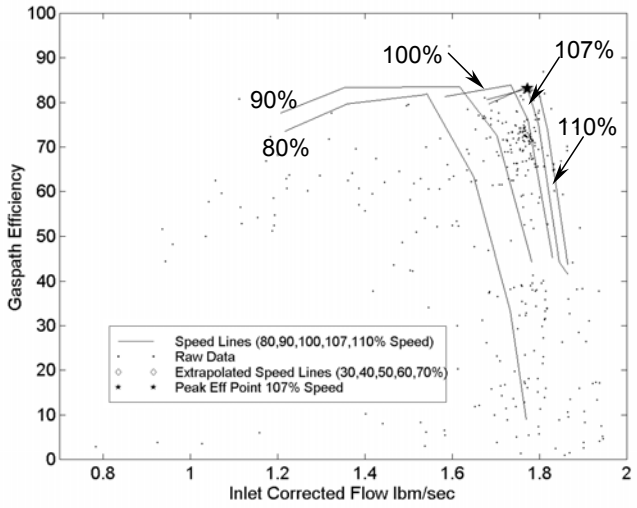

Figure 8. Compressor Efficiency Map

flow-path or any other system losses – this plot shows adiabatic compression efficiency of the supersonic rotor gas-path only. These characteristics were generated with relatively tight tip clearances. The star on Figure 8 is a point indicating the peak

efficiency achieved by the system during tests conducted to date.

The peak efficiency of any compressor is an important feature but sometimes the "off-design" performance characteristics are just as important. As indicated in Figure 8 shows, the efficiency of the rotor does not drop-off significantly at decreased rotor speeds and corrected flows. This is important for systems that must spend a significant amount of time operating at less than 100% speed or pressure ratio.

CO_2 COMPRESSOR DESIGN

The emergence of CO_2 as a key greenhouse gas contributing to global warming has intensified the focus on CO_2 sequestration systems to capture CO_2 when it is produced at power plants utilizing combustion. Many plans have been proposed for techniques of then storing or disposing of the CO_2. One approach is to compress and liquefy the gas so that it can be injected into saline aquifers beneath the sea floor. This technique can be used to store vast amounts of CO_2 and prevent its escape into the atmosphere, but this process requires large scale compression of CO_2 to very high pressures. Current CO_2 compression systems proposed for this application achieve overall pressure ratios on the order of 200:1. Figure 9 shows one such system. The compressor shown in Figure 9 is a ten stage unit that utilizes inter-cooling between each stage.

Figure 10 shows the pressure-temperature curve for the compression process utilized by the compressor shown in

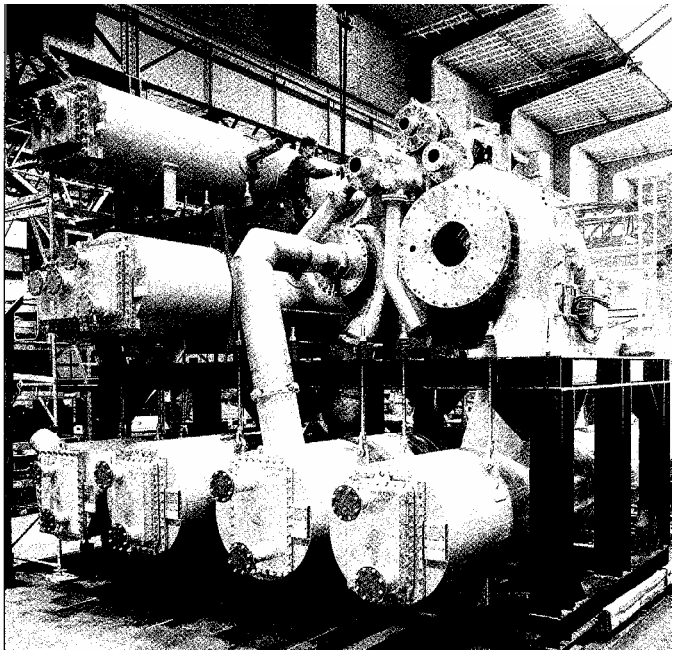

Figure 9. 10 Stage Intercooled CO_2 Compressor

Figure 9. The suction conditions are labeled S and the discharge conditions are labeled D. The need for conventional turbo-compressors that utilize centrifugal compression stages to limit the relative Mach numbers at the impeller inflow plane results in the relatively large size and number of stages required for this application.

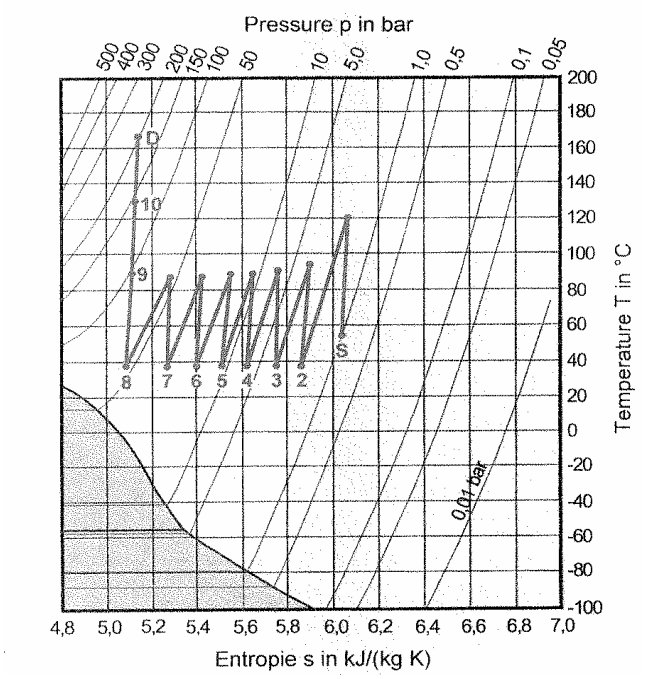

Figure 10. T-s Diagram for Compressor System

Since the Rampressor compressor depends on supersonic flow at the rotor inflow plane a significant size savings is available for a Rampressor system capable of delivering the same pressure ratios and flow rates as the compressor shown in Figure 9. Table 4 summarizes the key features of five system designs that could achieve the pressure ratios and mass flows as indicated in Figure 10 or other systems for CO_2 sequestration applications. As indicated in Table 4, Rampressor designs with two and three stages have been proposed for this application.

Table 4. Candidate System Summary

	Rampressor Systems			*Conventional Systems*	
Case	***1***	***2***	***3***	***4***	***5***
No. of Stages	*2*	*2*	*3*	*6*	*10*
Pressure Ratio	*45*	*200*	*200*	*45*	*200*
Inlet Water Temp (K)	*303*	*300*	*300*	*303*	*303*
P_{in} (kPa)	*187.5*	*99.9*	*99.9*	*187.5*	*99.9*
P_{out} (kPa)	*8,377*	*19,989*	*19,989*	*8,377*	*19,989*
Mass Flow (kg/s)	*89.51*	*10.56*	*10.56*	*89.51*	*10.81*
Volumetric In-Flow (m^3/s)	*29.02*	*6.31*	*6.29*	*29.00*	*6.52*
Drive Power (kW)	*28,614*	*5,130*	*4,538*	*28,818*	*4,695*
BHP/100	*61.62*	*49.79*	*44.04*	*62.90*	*45.57*
Isothermal Eff.	*0.7342*	*0.6733*	*0.7612*	*0.7169*	*0.7357*

The maximum stage pressure ratio required among the three proposed supersonic stages would be for case 2 and would be 14.1:1. This would result in the nominal 200:1 system pressure ratio being achieved in just two stages. The low speed of sound of CO_2 makes this possible with a rotor relative Mach number of ~2.42.

The cumulative losses of the multiple centrifugal stages required by the conventional system result in a relatively low overall efficiency. As indicated in Table 4, based on test results from the initial test program and analysis techniques validated by that program, an isothermal system of efficiency of 67% is

projected for the proposed two stage system and 76% for the three stage Rampressor system.

SUMMARY AND CONCLUSIONS

A proof-of-concept version of a novel supersonic compression stage has been designed, developed and tested. This stage applies supersonic aerodynamics design practices that are common in flight propulsion applications to the land based compression of a working gas.

Initial tests have shown that the stage starts and achieves peak performance levels that are consistent with the analytical models used to design the system. Testing indicates that the stage has benign un-start or surge characteristics and a nearly vertical full speed compressor characteristic. Because of the high stage pressure ratio, the system performance is sensitive to tip gap. The lessons learned in the design and operation of this rig are being applied to the design of a rig capable of operating at the increased speeds required to achieve the 9.9:1 pressure ratio.

The design tools and techniques validated by this effort have been used to perform the conceptual design of three supersonic compression systems that could be used for large scale CO_2 Compression. The results show that two and three stage compressor systems could be developed that would achieve pressure ratios of 200:1 when operating on CO_2 gas. Such compressors would be more compact, less expensive and more efficient than competing turbo-compressors utilizing multiple centrifugal stages.

ACKNOWLEDGMENTS

This effort was funded in part by the Department of Energy under the cooperative agreement #DE-FC26 00NT40, awarded between the period of October 1, 2003 and September 30, 2004.

REFERENCES

[1] Kerrebrock, J., Drela, M., Merchant, A., Shuler, B., 1998, "A family of designs for aspirated compressors", 98-GT-196.

[2] Jacklitch, J., Hartmann, M., 1953, "Investigation of 16-inch impulse-type supersonic compressor rotor with turning", NACA RM E53D13.

[3] Kantrowitz, A., 1948, "The supersonic axial flow compressor", Langley Aeronautical Laboratory Report 974.

[4] Simon, H., 1973, "A contribution to the theoretical and experimental examination of the flow through plane supersonic deceleration cascades and supersonic compressor rotors", Journal of Engineering for Power.

[5] Wilcox, W., Tysl, E., Hartmann, M., 1959, "Resume of the supersonic-compressor research at NACA Lewis Laboratory", Journal of Basic Engineering.

[6] Wright, L., Klapproth, J., 1949, "Performance of supersonic axial-flow compressors based on one dimensional analysis", NACA RM No. E8L10.

[7] Seddon, J., Goldsmith, E. L., *Intake Aerodynamics – Second Edition*, American Institute of Aeronautics and Astronautics, Virginia, 1999.

[8] Mahoney, J. J., *Inlets for Supersonic Missiles*, American Institute of Aeronautics and Astronautics, Washington, DC, 1990.

[9] Billig, F., Van Wie, D., 1987, "Efficiency parameters for inlets operating at hypersonic speeds", Eighth International Symposium on Air-Breathing Engines: p. 118-130.

[10] Wasserbauer, J., Meleason, E., Burstadt, P., 1996, Experimental investigation of the performance of a Mach-2.7 two-dimensional bifurcated duct inlet with 30 percent internal contraction, NASA TM-106728.

[11] Japikse, D., *Handbook of Fluid Dynamics and Fluid Machinery*, Volume 3, John Wiley & Sons, New York, 1996.